IR Thermometer with Automatic Emissivity Correction

Aleš DOBESCH, Juraj POLIAK

Dept. of Radio Electronics, Brno University of Technology, Purkyňova 118, 612 00 Brno, Czech Republic

xdobes05@stud.feec.vutbr.cz

Abstract. *The paper describes the design and implementation of an infrared (IR) thermometer with automatic emissivity correction. The temperature measurement is carried out by the simple digital thermopile sensor MLX90614. The emissivity correction is based on benefits of diffuse reflecting materials and it uses an IR laser diode in conjunction with a selective amplifier. Moreover, the paper includes the design of the control interface with a graphics LCD. Furthermore, this paper describes the power supply unit with a Li-ion cell controlled by basic integrated circuits.*

Keywords

Temperature, non-contact temperature measurement, emissivity, reflectivity.

1. Introduction

Non-contact temperature measurement has been quite a well-known method for a long time and nowadays, it is more and more the preferred method. The application of this method can usually be found in industrial branches such as engineering and metallurgy, but also in medicine and gastronomy [1]. There are many advantages of this non-contact method compared to the classical contact method. For example, fast measuring response, relatively wide measuring temperature range, the possibility of measuring moving parts, etc.

On the market there exists a wide spectrum of IR thermometer types; professional and expensive thermometers [2] as well as small and cheap ones [1]. However, in both cases the choice of non-contact automatic emissivity correction is missing.

The thermometer should have its own internal emissivity library combined with the possibility of manual emissivity settings. In addition, the thermometer should, as a unique feature, offer an automatic emissivity correction mode. Also, a control program in C should be written.

There is emphasis on using off-shelf components. The integrated thermopile sensor is suitable for temperature measurements. The automatic emissivity correction function can be realized by the reflection measuring circuit with an IR laser diode.

Section 2 introduces the theoretical background of the paper. Section 3 then presents the design of the device itself. Section 4 demonstrates the experimental solutions and measurements. Finally, the last section summarizes the results.

2. Theory

Any entity with a thermodynamic temperature T above 0 K is a source of electromagnetic radiation. The spectral range of this radiance lies between 0.4-25 μm and these wavelengths cover a measured temperature range between - 70 °C and 10 000 °C. Thus, the principle of the non-contact measurement is based on the conversion of the IR radiation to an electrically measurable unit.

2.1 Blackbody

A Blackbody is a physical model that is used to describe radiant behavior of a real object. The Blackbody is an idealized physical body that absorbs all radiation incident on it and reflects energy which is determined by the radiating system only and independent from the type of radiation which is incident on it. The peak of the possible radiated energy is dependent only on temperature. The Blackbody radiation covers the entire spectrum in order to absorb radiation regardless of its wavelength.

A physical quantity that characterizes the relative ability of a surface to emit thermal radiation is defined as emissivity ε. It is defined as the ratio of the energy radiated by a particular material to the energy radiated by the Blackbody at the same temperature.

$$\varepsilon(\lambda,T)=\frac{I_{\mathrm{e}}(\lambda,T)}{I_{\mathrm{eB}}(\lambda,T)} \tag{1}$$

where $I_{\mathrm{e}}(\lambda,T)$ is radiant intensity emitted by a real object ($[I_{\mathrm{e}}(\lambda,T)] = \mathrm{W/m^2}$) and $I_{\mathrm{eB}}(\lambda,T)$ is radiant intensity emitted by a Blackbody ($[I_{\mathrm{eB}}(\lambda,T)] = \mathrm{W/m^2}$).

According to (1) the emissivity ε of the Blackbody is 1. To describe a real object, a Graybody model is used. In this case the emissivity is a positive number smaller than 1.

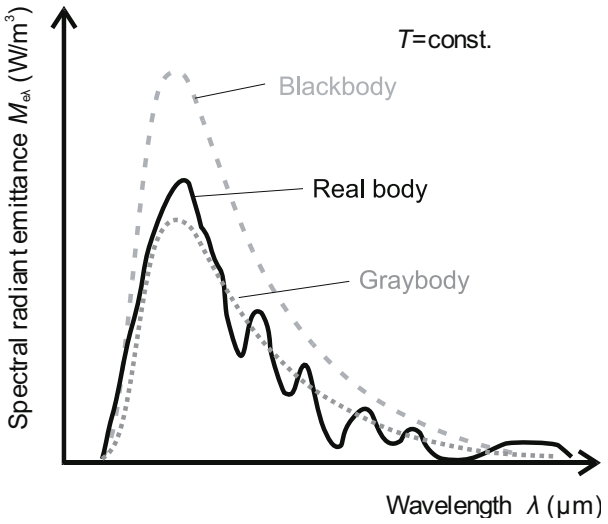

Fig. 1. Blackbody, Graybody and Real object radiance.

The emissivity of the surface changes and it is dependent on wavelength. The comparison of Blackbody, Graybody and the real body radiance is in Fig. 1 (inspired by [3]) and described in detail in following subsections.

2.2 Stefan–Boltzmann, Wien's Displacement and Planck's Law

The Stefan-Boltzmann law describes the power radiated from the Blackbody in terms of its temperature. According to (2), the total energy radiated per unit surface area of the Blackbody M_e across all wavelengths per unit time is directly proportional to the fourth power of the Blackbody thermodynamic temperature T,

$$M_e = \sigma \cdot T^4 \tag{2}$$

where σ = 5.67·10^{-8} W·m^{-2}·K^{-4} is Stefan-Boltzmann's constant and T is the thermodynamic temperature.

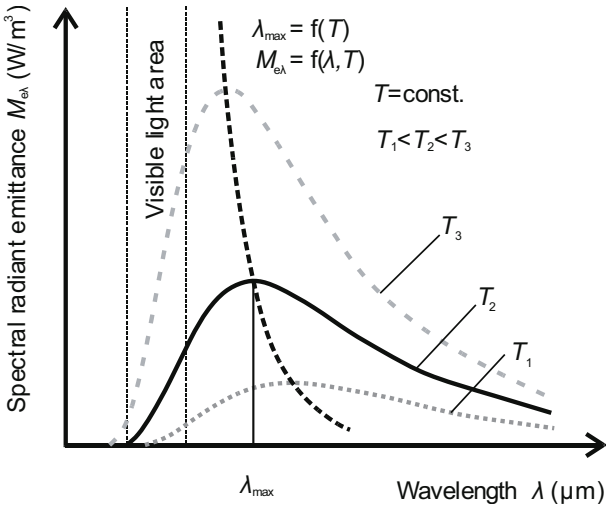

Fig. 2. Spectral radiant emittance dependent on wavelength.

As the temperature increases, the peak wavelength λ_{max} emitted by the Blackbody decreases to shorter wavelengths. This phenomenon is known as Wien's displacement law and mathematically can be expressed by (3),

$$\lambda_{max} = \frac{b}{T} \tag{3}$$

where b = 2.9·10^{-3} m·K is Wien's constant.

The most important equation (4) that explains the spectral-energy distribution of radiation emitted by the Blackbody is known as Planck's radiation law,

$$\mathrm{d}M_e = \frac{\hbar}{\pi^2 \cdot c^2} \cdot \frac{\omega^3}{e^{\frac{\hbar \cdot \omega}{k \cdot T}} - 1} \cdot \mathrm{d}\omega \tag{4}$$

where ω is angular frequency ([ω] = s^{-1}), $\hbar$ = 1.055·10^{-34} J·s is reduced Planck constant, c = 299 792 458 m·s^{-1} is the speed of light and k = 1.38·10^{-23} J·K^{-1} is Boltzmann constant. All three cardinal laws put together are illustrated in Fig. 2 (inspired by [4]).

2.3 Kirchhoff's Law of Thermal Radiation

The Kirchhoff's law of thermal radiation (5) states that the ratio of total thermal radiant intensity M_e to its dimensionless coefficient of absorption α is proportional to a universal function of thermodynamic temperature T,

$$\frac{M_e}{\alpha} = f(T)\,. \tag{5}$$

Long-wave IR radiation emitted by a body is composed of three radiant components, namely of emissivity ε, reflectivity ρ and transmissivity τ. The relation between these components is expressed by

$$\varepsilon + \tau + \rho = 1\,. \tag{6}$$

In a real case, the influence of the transmissivity τ is negligible. Thus, it can be omitted. Due to this fact, the final equation yields [4]

$$\varepsilon + \rho = 1\,. \tag{7}$$

2.4 Lambert's Cosine Law

In fact, the real object should be described as a selective radiant. Lambert's cosine law says that the radiant intensity I_e of a planar isotropic emitter observed from an ideal diffusely reflecting surface or ideal diffuse radiator is directly proportional to the cosine of the angle θ between the observer's line of sight and the surface normal.

This fact is expressed by [5]

$$I_e = I_n \cdot \cos(\theta) \tag{8}$$

where I_n is radiant intensity ([I_n] = W·sr^{-1}) and θ is angle of deviation from normal. This gives rise to selective radiation.

3. Design

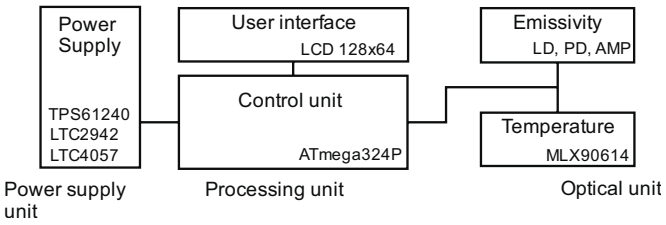

Fig. 3. The block diagram of an IR thermometer.

In Fig. 3, the complete block diagram of an IR thermometer is shown. The hardware is divided into three functional units – optical unit (temperature and emissivity sensors), processing unit and power supply unit. The most important component of the processing unit is the microcontroller ATmega324P. Temperature measurement is carried out by the digital IR thermopile sensor MLX90614. Emissivity measurement is implemented in a selective receiver and an IR laser diode at a wavelength of 850 nm. The key part of the power supply unit is the Li-ion cell together with special integrated circuits for charging, monitoring and voltage conversion.

3.1 Optical Unit

For precise temperature measurement it is important to know the target surface emissivity which corresponds to the radiant temperature. The true material emissivity value is changing dynamically and is dependent on the physical and chemical properties of the material. Very few materials and applications have a fixed emissivity [1]. Figure 4 shows dynamically measured true temperature.

Based upon the knowledge of Kirchhoff's law of thermal radiation and Lambert's law for diffused surfaces, it is possible to determine the emissivity ε by the known surface reflectivity ρ according to (7) and to calibrate the system accordingly. Fig. 5 shows the block diagram of the reflectivity measurement system.

The transmitter consists of an IR laser diode and a collimating lens. The collimated optical beam is Pulse Width Modulated (PWM) at 1.019 kHz. In general, the signal is modulated to suppress ambient noise hence improve sensitivity. The receiving part of the reflectance measurement system is carried out by a selective amplifier. The receiving optic focuses the light on a PIN photodiode. The photodiode is with a very small dark current and the maximum spectral sensitivity at 850 nm. As a transimpedance amplifier, a very low noise voltage operational rail-to-rail amplifier is used. The band-pass filter uses the benefits of a multiple feedback filter configuration. The programmable gain amplifier adjusts the level of the signal for Analog-Digital (AD) converter. The peak value of the output signal is processed in AD converter integrated in the microcontroller ATmega324P.

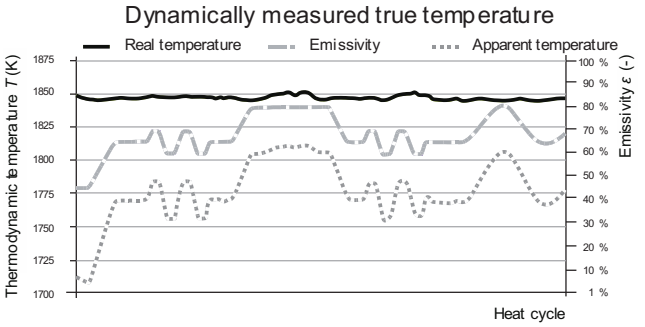

Fig. 4. Dynamically measured true temperature [1].

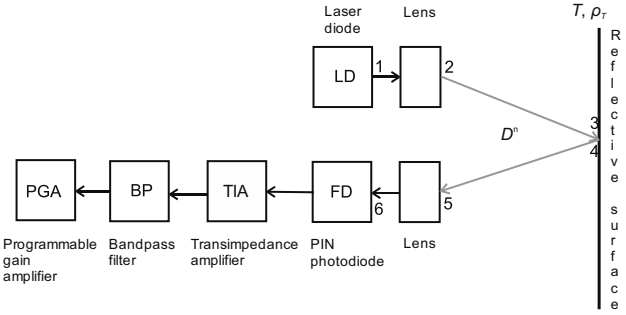

Fig. 5. The block diagram of the reflectance measurement system.

A. Emissivity measurement

In the case of a diffusely reflecting surface and perpendicular measurement, the target reflectivity ρ_T can be measured using the calibration method according to (9). At the beginning, the reflectance measuring system is calibrated by the surface with known target reflectivity ρ_T. Using this calibration measurement the receiver voltage sensitivity S_U (given in V/W) is obtained. This value is saved in the system memory. Then the reflectance of other surfaces based on detected voltage U_{det} with respect to S_U can be determined. The resulting value of emissivity ε can be calculated according to (7). Finally,

$$\rho_T = \frac{4 \cdot U_{det} \cdot D^n}{S_U \cdot P_L \cdot d^2} \cdot \eta_{sys} \tag{9}$$

where D is measured object distance, P_L is laser diode power, d is diameter of receiving area ([d] = m), n is an approximation coefficient of the distance power function and η_{sys} is system calibration distance constant ([η_{sys}] = m^{2-n}).

Resulting from (9), there is a need to accurately measure the distance of the target object. There are at least two commonly used choices. The first one is the Time of Flight (TOF) method that covers a variety of methods used to measure the time that it takes for an optical signal to reach an object.

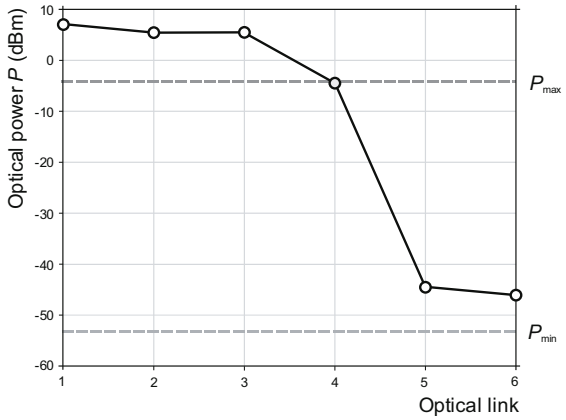

Fig. 6. Link budget.

The disadvantage of this method is very hard implementation. Due to this fact, the triangulation distance ranging method is used. Triangulation is a process of determining the location of a point by angle measurement. The second method is used in this work at the expense of accuracy and distance limitation. Considering the simplicity, a SHARP integrated distance sensor is used. To determine a required dynamic range of the reflectance measurement system receiver, the optical link budget is calculated and simulated (cf. Fig.6). Individual points 1-6 in Fig. 6 represent the gains and losses between the transmitter and the receiver. The first point presents the laser diode optical output power. Point 2 expresses the optical coupling losses between the laser diode and an optical lens. The attenuation of spreading is in point 3. Point 4 presents the attenuation of the surface absorption. In point 5, optical power is received by the optical system. The last sixth point presents the PIN photodiode received power [1], [6], [7], [8].

In Fig. 6, borders of the maximum and minimum optical system power *P* are also marked. Obviously the highest losses are evident between points 4 and 5. These two points correspond to surface absorption and reflected radiation from the diffused surface respectively.

B. Temperature measurement

The temperature measurement is carried out by means of an MLX90614 sensor. This one zone calibrated digital sensor consists of two integrated circuits. The first one is MLX81101 IR thermopile and the second one is the Digital Signal Processor (DSP) that processes the IR thermopile output signal. Also, it contains a bank of digital filters. The measuring range of this non-contact sensor covers temperatures between -70 °C and 380 °C. The producer also offers custom sensor variations with a range of up to 1030 °C.

The sensor offers two possibilities of communication with the microcontroller. An SMBus protocol or a direct PWM sensor output can be used. The SMBus protocol is preferred thanks to easier registry access and internal sensor setting.

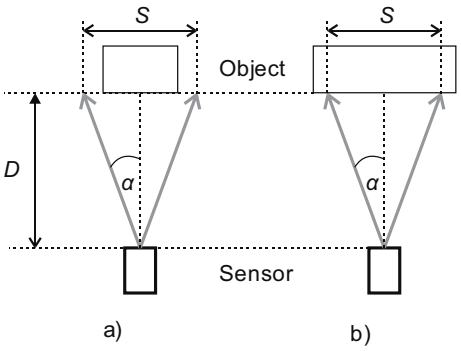

Fig. 7. Field of view. a) wrong and b) correct measurement setup.

In order to perform a correct measurement, condition (10) must be fulfilled,

$$S = 2 \cdot D \cdot \tan(\alpha) \tag{10}$$

where α is the field of view (FOV) of the sensor (cf. Fig. 7).

The MLX90614 sensor is manufactured in many variants of FOV. The variant with the smallest viewing angle provides 10°. To narrow the FOV of the sensor and so improve the measurement distance *D,* special Fresnel lenses are commonly used.

3.2 Processing Unit

The crucial part of the IR thermometer is the microcontroller Atmega324P with an accurate clock frequency of 8 MHz, which is provided by an external crystal oscillator. Communication with both thermopile sensor MLX9014 and battery gas gauge is handled via a two-wire SMBus protocol. The bus clock frequency is set to 100 kHz.

A 16-bit internal timer/counter generates a precisely modulated 1.019 kHz signal. The timer output switches JFET n-channel transistor for IR laser diode driving.

A 10-bit internal AD converter handles the analog input signal from both the selective receiver and SHARP integrated rangefinder sensor. The output processed data is displayed on a graphic LCD. Three tactile switches are used for easy control and simple menu navigation of the IR thermometer.

3.3 Power Supply Unit

An IR non-contact thermometer is considered to be a portable device. Hence, a Li-ion cell with a nominal voltage of 3.6 V is used. It is the most popular secondary cell type for portable devices for its high energy density, no memory effect, low self-discharge rate and relatively small weight. A small disadvantage is that a potential damage can occur. Hence, the protecting circuits must be a part of the power supply with a Li-ion cell. Figure 8 shows the circuit diagram of the battery management.

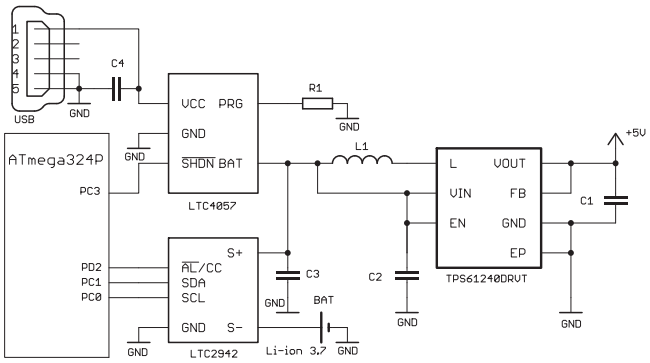

Fig. 8. Power unit schematic.

The integrated circuit LTC4057 is a USB stand-alone single-cell constant-current/constant-voltage linear charger for Li-ion batteries. The maximum charging current is 420 mA. When the input power supply is removed, the LTC4057 automatically enters into a low current sleep mode.

Another integrated circuit, LTC2942-1, has a battery gas gauge with temperature and voltage measurement. This circuit communicates with the microcontroller ATmega324P via the SMBus protocol. The main task is to monitor the Li-ion cell temperature, total accumulated energy and the voltage level.

The Li-ion voltage level fluctuates between 2.8 and 4.2 V. Therefore, a synchronous step-up DC-DC converter with efficiency up to 90 % optimized for products powered by battery cells is used. The switching frequency is 3.5 MHz. The maximum output current 450 mA is sufficient.

4. Experimental Verification

	Reference	Chalk	Mortar	Polystyrene	Black paper
Table emissivity	0.68	0.70	0.80	0.64	0.94
Measured emissivity	0.68	0.70	0.76	0.70	0.94

Tab. 1. Experimentally measured emissivity values.

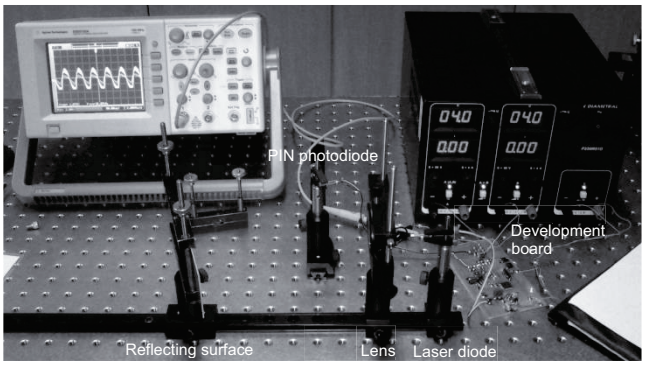

Fig. 9. The experimental emissivity measurement system.

In Tab. 1, there is a comparison of emissivity table values of the basic materials with emissivity values measured experimentally using the proposed method. The emissivity is measured with a precision of 2 %. Some values may differ because of imperfect surface preparation.

Figure 9 shows an experimental emissivity measuring system with a development board. By using this experimental system, the functionality of the non-contact emissivity measurement method was confirmed. For precise emissivity measurements, high accuracy of distance measurement is necessary.

In Fig. 10, the comparison of contact and non-contact temperature measurement is shown. The dashed gray line presents the temperature measurement with a high precision contact thermometer. The dotted gray line demonstrates non-contact temperature measurement with a common IR thermometer with firm emissivity setting at 0.95. The black line shows the non-contact temperature measurement carried out using the IR thermometer prototype with emissivity correction. Inaccuracy caused by the firm emissivity setting is obvious. The difference between both non-contact measurements is up to 18 K. The ability of non-contact emissivity correction and therefore better temperature measurement accuracy is the main contribution of this work. Polystyrene is used as an experimental measurement sample. The reference surface of emissivity measurement is a white paper with exactly known reflectivity $\rho_T = 0.32$.

Figure 11 illustrates the IR thermometer control unit on the right- and the measurement front panel on the left-hand side. Also, all built-in sensors are distinctly marked in Fig. 11.

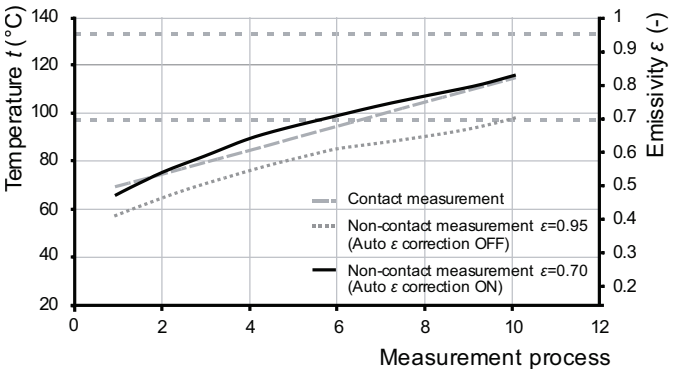

Fig. 10. Temperature measurement accuracy.

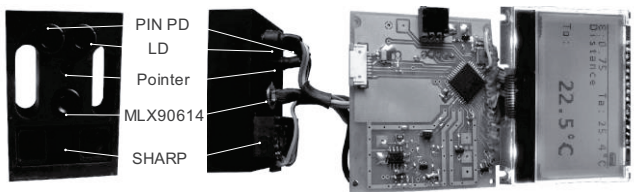

Fig. 11. Control unit and front panel.

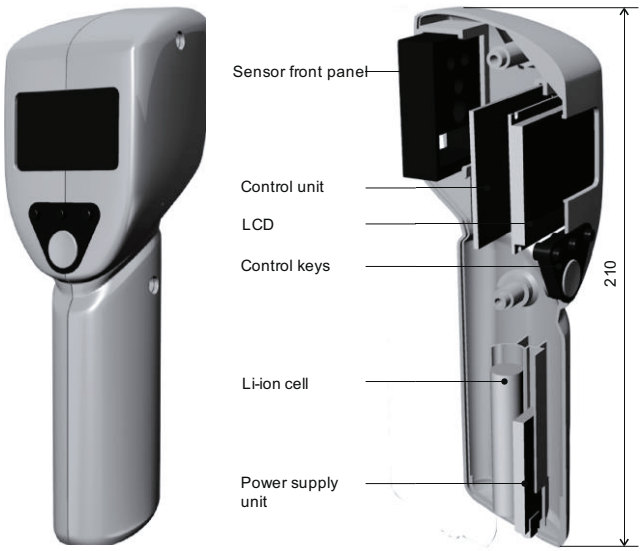

Fig. 12. Design of IR thermometer prototype.

In Fig. 12, a prototype model of the IR thermometer is shown. The body is printed on a 3D printer using ABS plastic. Furthermore, the inner placement of electronic components is shown.

5. Conclusion

This paper describes the basic facts and laws that stand behind the IR non-contact temperature measurement. However, the crucial part of this paper is focused on non-contact emissivity measurement. The main problem of the importance of emissivity determination is explained. Based on detailed theoretical and experimental knowledge, the system of non-contact emissivity correction is designed. The precise implementation of the emissivity measurement system is supported by both simulation and experimental verification.

The complete optical unit consists of non-contact emissivity correction and a simple IR sensor MLX90614 for non-contact temperature measurement. The control unit is formed by an 8-bit microcontroller with a large graphic LCD together with four tactile switches. As a power supply, a Li-ion cell with protection and charging circuits is used. The ABS body of the IR thermometer is printed on a prototype 3D printer.

The possibility and correctness of the non-contact emissivity measuring method was confirmed. However, the calibration method is limited by some aspects. The first one is the necessity of the diffused character of the measured surface and the requirement to measure perpendicularly. Also, special attention should be paid to the design of the distance measurement unit.

Acknowledgements

This paper was supported by the project CZ.1.07/2.3.00/20.0007 WICOMT, the operational program Education for Competitiveness. Measurements were performed in the laboratories supported by the SIX project; the registration number CZ.1.05/2.1.00/03.0072, the operational program Research and Development for Innovation. The research is a part of the EU COST Action IC1101 and financially supported by the Czech Ministry of Education under grant no. LD12067 and by the Czech Ministry of Industry and Trade under grant agreement No. FR-TI4/148 and No. FR-TI2/705.

References

[1] FLUKE. *IR Thermometers.* [Online] Cited 2012-05-08. Available at: http://www.fluke.com/fluke/czcs/products/Teplomery.htm.

[2] PYRO. *Real Time Emissivity Measurement For Infrared Temperature Measurement.* [Online] Cited 2012-05-08. Available at: http://www.pyrometer.com/pyro_technology.html.

[3] MASSOUD, M. *Engineering Thermofluids: Thermodynamics, Fluid Mechanics, and Heat Transfer*. Berlin (Germany): Springer, 2005.

[4] Omega Engineering. *Zpravodaj pro měření a regulaci.* [Online] Cited 2012-05-08. Available at: http://www.omegaeng.cz/literature/PDF/techinfo_1.pdf

[5] SMITH, W. J. *Modern Optical Engineering: The Design of Optical Systems.* New York (USA): McGraw Hill, 2000.

[6] JEN, D. C. *Radar and Laser Cross Section Engineering*, 2nd ed. Reston (VA,USA): AIAA, 2005.

[7] JELALIAN, A. V. *Laser Radar Systems*. Boston (MA, USA): Artech Print on Demand, 1992.

[8] BENGTSSON, L. E. *Implementation of High-Resolution Time-to-Digital Converter in 8-bit Microcontrollers*. Gothenburg (Sweden): Department of Physics, University of Gothenburg, 2012.

About Authors …

Aleš DOBESCH was born in 1989. He received his Ing. (M.Sc.) degree in Electrical Engineering in 2013 and currently is a PhD student at the Department of Radio Electronics, Brno University of Technology. His main focus is modeling and experimental verification of optical measurement techniques. He is also specialized in modeling and simulating LED radiation distribution and optical communication systems design.

Juraj POLIAK was born in 1987. He received his Ing. (M.Sc.) degree in Electrical Engineering in 2011 and currently is a PhD student at the Department of Radio Electronics, Brno University of Technology. His main focus is on modeling laser beam behavior along the propagation path and the influence of various phenomena on its intensity profile. He is also a member of SPIE and IEEE.